Measurement of ionization and recombination rates for Fe XVI – Fe XXII from time-resolved spectroscopy of tokamak plasmas

Jieh-Shan Wang, Hans R. Griem, and Roger Hess
Laboratory for Plasma and Fusion Energy Studies, University of Maryland, College Park, Maryland 20742

William L. Rowan
Fusion Research Center, University of Texas, Austin, Texas 78712
(Received 19 January 1988)

The effective ionization and recombination rate coefficients for Fe XVI–Fe XXII were obtained by studying the modulation of line emissions by sawtooth oscillations in the TEXT tokamak. Experimental data are matched with the simulation of iron ion emission by a one-dimensional code. The rate coefficients were determined for $T_e \sim 350$–900 eV and $N_e \sim (4$–$5.6)\times 10^{13}$ cm^{-3}. The rate coefficients for Fe XVI, XVII, and XVIII have large uncertainty partly due to uncertainty of the temperature profile at large radii of the plasma and partly due to other possible atomic processes. The error of ionization rates for Fe XIX–Fe XXII is estimated to be less than 40%, while the estimated accuracy of the recombination rates is better than a factor of 2.

I. INTRODUCTION

Ionization and recombination rate coefficients are important atomic data for calculations of the ionic balance in plasmas. In fusion plasmas the rates are required for studies of impurity transport and power balance. In laser produced plasmas, dense z-pinch plasmas and astrophysical plasmas, the rates are required for calculation of ionic abundances that are important for interpretation of observed radiation. The corresponding cross sections are often obtained from approximate theories, with experimental checks from crossed beam experiments being still rare and sometimes less direct than anticipated. Most direct measurements of atomic rate coefficients have been done in θ-pinch devices.[1,2] Because of the limitation in electron temperature, θ pinches can only be used to study ions of relatively low charge state. For highly ionized ions requiring higher electron temperature, measurements of effective rate coefficients can be done in tokamaks, the ions being an intrinsic impurity or introduced artificially. Breton *et al.*[3] measured ionization and recombination rates for Mo XXXI from observed sawtooth modulation of Mo XXXI and Mo XXXII line emissions. Isler *et al.*[4] measured ratios of ionization and recombination rates for Fe XV–Fe XIX in the ISX-B tokamak during counterinjection of neutral beams. Recently, Wang *et al.*[5,6] measured ionization and recombination rates for Ti XVII–Ti XX and Ar XII–Ar XVI. They extended the method of Breton *et al.* to include the effect of tokamak transport and temperature profile variation during the sawtooth cycle. Line emissions were simulated by a one-dimensional (1D) code, which takes into account the sawtooth temperature variation, for comparison with the experiment.

In this article we report the determination of ionization and recombination rate coefficients for highly ionized iron ions using the same method as described by Wang *et al.*[5] The principle of the measurement will be discussed only briefly in Sec. II as a more detailed discussion of the principle and numerical method can be found in Ref. 5. Section III contains the experimental parameters and a brief description of the experiment. Section IV contains results and discussions of our measurement.

II. PRINCIPLE OF THE MEASUREMENT

Sawtooth oscillations in the soft x-ray signal in a tokamak have been explained by the flattening and reheating of the electron temperature profile which may become flattened or even hollow at the center of the plasma.[7,8] The change of the T_e profile can, through ionization and recombination, change the relative abundances of impurity ions. This has been observed in the modulation of line emission signals. While the temperature profile can flatten for a short time, as seen from the rapid crash in the soft x-ray signals, the relative ionic abundances vary rather smoothly according to the processes of ionization and recombination. Thus one can observe time lags or phase differences between the line emission and soft x-ray signals. The phases are affected by the ionization and recombination rates, and one can obtain the atomic rates from the observed phase differences. However, in order for the coupling of atomic processes and the sawtooth activity to be effective, the atomic relaxation time should be comparable to the sawtooth period. Also, because the particle transport time scale is usually about one order of magnitude larger than the sawtooth period, the transport processes (i.e., diffusion and convection) are considered to be of less importance. Thus the exact knowledge of the transport coefficients is not necessary. Such assumption, however, does not apply to all the plasma conditions. As we will discuss in Sec. IV, there are conditions under which the particle transport time scale may be comparable to the sawtooth period and our method cannot be used anymore. There have been observations of anomalously large transport processes especially during the sawtooth crash phase.[9,10] Under such conditions the transport process during the sawtooth crash dominates other processes, and the line emission signals should be either in or out of phase with the soft x-ray signal. Though relative abundances of the impurities ions were changing due to atomic processes in the sawtooth rising phase, we can no longer determine the ionization and recombination rate coefficients.

The phase differences follow from the correlations

$$C(\tau)=\frac{\int_0^T S(t)L(t+\tau)dt}{\left[\int_0^T S(t)S(t)dt\right]^{1/2}\left[\int_0^T L(t)L(t)dt\right]^{1/2}}, \quad (1)$$

where $S(t)$ is the soft x-ray signal and $L(t)$ is the line emission signal.[11] A 1D code that solves the transport-ionization-recombination equations

$$\frac{\partial N_k}{\partial t}=-\frac{1}{r}\frac{\partial(r\Gamma_k)}{\partial r}+N_e(S_{k-1}N_{k-1}-S_kN_k+\alpha_{k+1}N_{k+1}-\alpha_kN_k) \quad (2)$$

calculates the ionic abundances. In the equation, the Γ_k's are the particle fluxes, the S_k's and the α_k's are the ionization and recombination rate coefficients, respectively. The particle fluxes are written as

$$\Gamma_k=-\left[D(r)\frac{\partial N_k}{\partial r}+V(r)N_k\right], \quad (3)$$

where $D(r)$ is the diffusion coefficient and $V(r)$ is the convective velocity, both assumed to be independent of the ion species. The diffusion coefficient is assumed to be constant at 10^4 cm^2/s. The convective velocity is assumed to be of the form $V(r)=V(a)(r/a)$, with $V(a)=10^3$ cm/s, and $a=27$ cm is the minor radius. These transport coefficients were measured using the impurity-injection method.[12] A sawtooth function inferred from the soft x-ray measurements[13] is used to generate variations of the temperature profile which in turn causes variations in the rate coefficients. The assumed average temperature profile is consistent with Thomson scattering, electron cyclotron emission and soft x-ray diode array measurements.

The ionization rate coefficients are calculated using Lotz's formula.[14] The recombination rate coefficients are the sum of the dielectronic rates from Burgess' formula[15] with a correction for $\Delta n>0$ transitions,[16,17] and the radiative rates are from a hydrogenic formula.[18] The rate coefficients are varied by adjustable multipliers.

Line emissions are calculated from the ionic abundance profiles which are solutions of the equations. The correlations with the sawtooth function are then calculated using Eq. (1). These simulated correlations are compared with the experimental correlations. The rate coefficients are varied to achieve a better match of the two correlations. The rates are determined from the best match. Errors can be estimated from the sensitivity of the calculated correlations to the variation of the input parameters.

III. THE EXPERIMENT

The measurements of the iron ion rate coefficients were done on the TEXT tokamak. Two plasma conditions were studied in this experiment. One condition has plasma current of 300 kA and a toroidal magnetic field of 28 kG, and the other condition had plasma current of 200 kA and a toroidal magnetic field of 20 kG. However, only the first condition was suitable for our method. The second condition shows that the correlations for most of the ions are in phase. This result may have been due to anomalies in the impurity transport. The sawtooth amplitude for the second condition is about a factor of 2 larger than that of the first condition. We will discuss this result in Sec. IV. The plasma parameters described in the next few paragraphs are only for the first plasma condition.

Diagnostics for the experiment include electron cyclotron emission (ECE), the TEXT silicon surface barrier diode array, microwave interferometry, and vuv spectroscopy. The iron atoms are natural impurities from the stainless steel vacuum chamber. The line averaged electron density was measured by microwave interferometry to be $\sim 4.5\times10^{13}$ cm^{-3}. The sawtooth oscillation had an average period of ~ 5.0 ms. The period varied between 4.5 and 6 ms. The average electron temperature profile is of the form $T_e(r)=T_e(0)\exp[-(r/b)^c]$, where $T_e(0)=900$ eV, $b=16.1$ cm, and $c=2.5$. The electron density profile is of the form

$$N_e(r)=N_e(0)\{0.9[1-(r/a)^2]+0.1\} .$$

We used a 2.2-m grazing incidence monochromator, and a 1-m normal incidence monochromator. The observed iron ion spectral lines are listed in Table I. The spectrometers view the plasma along a central chord.

The correlations of line emission signals with the soft x-ray signal are shown in Figs. 1(a) and 2(a), the quantity θ in the figures is the phase shift. Because of high noise levels the normalized correlations have amplitudes of about 0.3 to 0.5. The background, where no spectral line was observed, however, has correlation amplitudes of less than 0.1.

IV. RESULTS AND DISCUSSION

Figures 1(b) and 2(b) show the matching simulated correlations. Effective ionization and recombination rate coefficients corresponding to this match are listed in Tables II and III, respectively. The electron temperatures listed in the tables are the values at the radius where each ion has its peak abundance. However, the ratios between experimental ($\alpha^t_{\rm eff}$) and theoretical rate coefficients ($\alpha^r+\alpha^d_{\rm th}$) are the same at all radii. Rates from theoretical calculations are also listed in Tables II and IV for comparison with our measurement.

Errors of the rate coefficients can be estimated by checking the sensitivity of the simulated correlations to the assumed values. It is found that a $\pm40\%$ simultaneous variation of all the ionization rates can cause phase changes of about 0.5 rad, which is larger than the errors in the experimental phases. The correlations of Fe XVIII and Fe XXI are sensitive to the change of recombination rates to within 60% variation. The other correlations are less sensitive to the changes in recombination rates.

TABLE I. Observed spectral lines.

Ion	Lines (Å)	Transitions
Fe XVI	360.8	$3s(^2S_{1/2})$-$3p(^2P_{1/2})$
Fe XVII	243.4	$2p^5(^2P_{1/2})3s(\frac{1}{2},\frac{1}{2})^0_1$-$2p^5(^2P_{1/2})3p(^1S_0)$
Fe XVIII	974.8	$2s^22p^5(^2P_{3/2})$-$2p^5(^2P_{1/2})$
Fe XIX	1118.1	$2s^22p^4(^3P_2)$-$2p^4(^3P_1)$
Fe XX	2665.1	$2s^22p^3(^2D_{3/2})$-$2p^3(^2D_{5/2})$
Fe XXI	1354.1	$2s^22p^2(^3P_0)$-$2p^2(^3P_1)$
Fe XXII	845.5	$2s^22p(^2P_{1/2})$-$2p(^2P_{3/2})$

Simultaneous variation of all these rates by a factor of 2 also causes significant changes in the correlations. Such tests give an estimation of errors of the ionization and recombination rate coefficients.

The transport coefficients are not critical in the analysis of our first condition. Detectable changes in the correlations require a variation of more than a factor of 2 of the values that were used.

For the second experimental condition, in which the phases of the correlations are the same, we did not find any matching solutions with fixed transport coefficients. We have to note that the sawtooth amplitude of this condition is twice as large as for the first condition. This may suggest that the transport processes may be different from what we have assumed in our analysis. If the transport processes become dominant, the correlations are no longer controlled by ionization and recombination. Thus we cannot determine the rates in this case.

The ionization rate coefficients for Fe XIX, Fe XX, Fe XXI, and Fe XXII are in agreement with semiempirical value of Lotz,[14] and theoretical values of Golden and Sampson.[19] But the ionization rates for Fe XVI, Fe XVII, and Fe XVIII are considerably larger than Lotz's values. Since these ions exist mostly at large radii, it might be that the temperature profile used in our calculation is not correct, although a significantly different temperature profile, exceeding experimental errors, is needed to account for the discrepancy. Another possible reason for high ionization rates are processes such as autoionization following excitation and the existence of excited metastable states for these ions. Because of low electron and ion

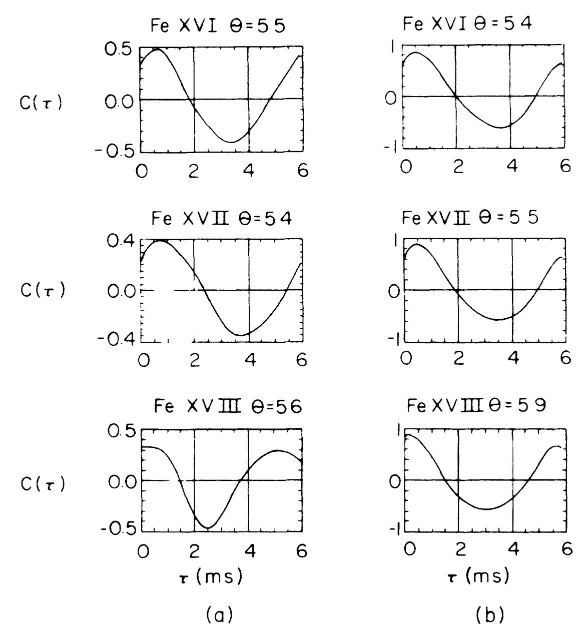

FIG. 1. (a) Experimental correlations for Fe XVI–Fe XVIII. (b) Calculated correlations. θ is the phase shift.

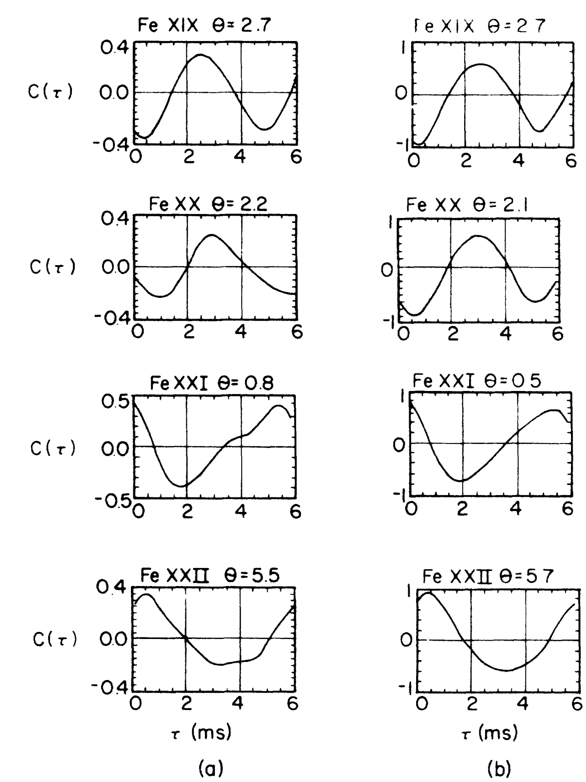

FIG. 2. (a) Experimental correlations for Fe XIX–Fe XXII. (b) Calculated correlations. θ is the phase shift.

TABLE II. Effective ionization rate coefficients (10^{-11} $cm^3 s^{-1}$).

Ion	kT_e (eV)	N_e (10^{13} cm^{-3})	S_{expt}	Lotz[a]	GS[b]	GPB[c]
Fe XVI	350	4.0	15.8	4.1		14
Fe XVII	350	4.0	0.96	0.48		
Fe XVIII	350	4.0	0.88	0.31		
Fe XIX	650	4.8	1.5	1.5	1.8	
Fe XX	900	5.6	1.4	1.9	2.3	
Fe XXI	900	5.6	1.4	1.2	1.4	
Fe XXII	900	5.6	0.6	0.7	0.8	

[a]Lotz, Ref. 14.
[b]Golden and Sampson, Ref. 19.
[c]Griffin, Pindzola, and Bottcher, Ref. 22.

densities in this region the metastable states can exist for a long time, and effective ionization rates from these states can be larger than those for the ground state. Large contributions of excited states to the ionization rate coefficients have been observed in both cross-beam experiments[20] and plasma experiments.[21] Recent calculations by Griffin *et al.*[22] show there is a very large contribution of excitation autoionization to the ionization cross section. They calculated the ionization rate coefficient for Na-like Ti XII, Cr XIV, Fe XVI, and Ni XVIII. Their ionization rate coefficient for Fe XVI at 350 eV is about 1.4×10^{-10} $cm^3 s^{-1}$, which is in very good agreement with our measurement.

The dielectronic recombination rates for Fe XIX, Fe XX, and Fe XXI are within about 20% of the theoretical values α^d_{SS} of Shull and Van Steenberg[23] and values α^d_J of Jacobs *et al.*[24] For Fe XXII, the experimental value is about a factor of 2 less than the calculation of Jacobs *et al.* The dielectronic rate for Fe XIX is about 30% less than a recent calculation by Roszman.[25] The dielectronic recombination rates for Fe XVI, Fe XVII, and Fe XVIII may be considered unreliable, if we assume the ionization rates for these ions are uncertain as discussed in the last paragraph. Although the dielectronic rate for Fe XVI is a factor of 2 less than Shull and Van Steenberg's value, it is in good agreement with the calculation by Jacobs *et al.* For Fe XVIII the dielectronic rate coefficient is 30% larger than both theoretical values in Table IV, and it is smaller than the calculation of Roszman[26] by 50%. These discrepancies are within the experimental errors. The dielectronic rate coefficient for the neonlike Fe XVII is, nevertheless, significantly larger than all theoretical values. Table IV also lists dielectronic rates for Fe XVII, Fe XVIII, and Fe XIX obtained by Isler *et al.*[4] For Fe XVIII and Fe XIX the measurements appear to be in agreement with each other, while for Fe XVII our value is larger by a factor of 3. Most of this increase could be due to the larger ionization rate (see Table II) compared to the Lotz value which was used by Isler *et al.* as a reference in their determination of the ratio of recombination and ionization coefficients. If a corresponding correction were applied also to the values of Isler *et al.* for Fe XVIII

TABLE III. Effective recombination rate coefficients. α^t_{eff} is the effective recombination rate coefficient determined from our experiment. The measured dielectronic recombination rate coefficient α^d_{expt} is $\alpha^t_{eff}-\alpha^r$. α^r is the calculated radiative recombination rate coefficient. α^d_{th} is our calculation of the dielectronic rate coefficient using Burgess' formula. The rate coefficients are in units of 10^{-11} $cm^3 s^{-1}$.

Ion	kT_e (eV)	N_e (10^{13} cm^{-3})	α^t_{eff}	α^r	α^d_{expt}	α^d_{th}
Fe XVI	350	4.0	2.2	0.15	2.0	2.0
Fe XVII	350	4.0	3.9	0.2	3.7	2.6
Fe XVIII	350	4.0	2.3	0.2	2.1	1.1
Fe XIX	650	4.8	1.9	0.16	1.7	0.46
Fe XX	900	5.6	1.4	0.14	1.2	0.83
Fe XXI	900	5.6	1.4	0.2	1.2	0.8
Fe XXII	900	5.6	0.9	0.2	0.7	0.46

TABLE IV. Comparison of dielectronic recombination rate coefficients (10^{-11} $cm^3\,s^{-1}$).

Ion	kT_e (eV)	α^d_{expt}	JDKB[a]	SS[b]	R[c]	ICA[d]
Fe XVI	350	2.0	2.0	3.5		
Fe XVII	350	3.7	0.75	0.9		1.24
Fe XVIII	350	2.1	1.4	1.4	3.5	1.75
Fe XIX	650	1.7	1.5	1.3	2.4	1.50±0.45
Fe XX	900	1.2	1.2	1.4		
Fe XXI	900	1.2	1.4	1.2		
Fe XXII	900	0.7	1.7	0.5		

[a]Jacobs, Davis, Kepple, and Blaha, Ref. 24.
[b]Schull and Van Steenberg, Ref. 23.
[c]Roszman, Refs. 25 and 26.
[d]Isler, Crume, and Arnurius, Ref. 4. These rates are listed at $T_e = 480$ eV for Fe XVII and Fe XVIII, and at 680 eV for Fe XIX.

and Fe XIX, their recombination coefficients for these ions would exceed ours by a factor of about 2.

ACKNOWLEDGMENTS

We wish to thank A. J. Wootton, TEXT Director, for his cooperation during this experiment; K. W. Gentle, R. V. Bravenec, Burton Richard, and Kjell Nelin for operating TEXT; and the members of the TEXT Technical Staff for assisting in the setup. Two of us (J.S.W. and H.R.G.) wish to thank Dr. S. Goldsmith of Tel Aviv University for his suggestions. This work was supported by the U. S. Department of Energy.

[1]H. R. Griem, J. Quant. Spectrosc. Radiat. Transfer (to be published).
[2]H.-J. Kunze, Space Sci. Rev. **13**, 565 (1972).
[3]C. Breton, C. DeMichelis, M. Finkenthal, and M. Mattioli, Phys. Rev. Lett. **41**, 110 (1978).
[4]R. C. Isler, E. C. Crume, and D. E. Arnarius, Phys. Rev. A **26**, 2105 (1982).
[5]J. S. Wang, H. R. Griem, R. Hess, W. L. Rowan, and T. P. Kochanski, Phys. Rev. A **33**, 4293 (1986).
[6]J. S. Wang, H. R. Griem, and W. L. Rowan, Phys. Rev. A **36**, 951 (1987).
[7]S. von Goeler, W. Stodiek, and N. Sauthoff, Phys. Rev. Lett. **33**, 1201 (1974).
[8]F. Korgar *et al.*, in *Plasma Physics and Controlled Nuclear Fusion Research,* Proceedings of the Sixth Conference, Berchtesgaden, 1976 (IAEA, Vienna, 1977), Vol. I, 267.
[9]R. Petrasso, F. H. Seguin, N. G. Loter, E. Marmar, and J. Rice, Phys. Rev. Lett. **49**, 1826 (1982).
[10]TFR Group, Nucl. Fusion **25**, 981 (1985).
[11]W. D. Stanley, *Digital Signal Processing* (Reston Publishing, Reston, VA, 1975).
[12]W. L. Rowan *et al.*, Bull. Am. Phys. Soc. **28**, 1033 (1983).
[13]J. A. Snipes, T. P. Kochanski, and S. B. Kim, The University of Texas Fusion Research Center Report No. 225, 1983 (unpublished).
[14]W. Lotz, Institut für Plasmaphysik, Garching bei München, Report No. IPP 1/62, 1978 (unpublished).
[15]A. Burgess, Astrophys. J **141**, 1588 (1965).
[16]A. L. Merts, R. D. Cowan, and N. H. Magee Jr., Los Alamos Scientific Laboratory Report LA-6200-MS, 1976 (unpublished).
[17]R. D. Cowan, *The Theory of Atomic Structure and Spectra* (University of California Press, Berkeley, 1981).
[18]H. R. Griem, *Plasma Spectroscopy* (McGraw-Hill, New York, 1964).
[19]L. B. Golden and D. H. Sampson, J. Phys. B **10**, 2229 (1977).
[20]D. C. Gregory, F. W. Meyer, A. Müller, and P. Defrance, Phys. Rev. A **34**, 3657 (1986).
[21]R. U. Datla and J. R. Roberts, Phys. Rev. A **28**, 2201 (1983).
[22]D. C. Griffin, M. S. Pindzola, and C. Bottcher, Phys. Rev. A **36**, 3642 (1987).
[23]J. M. Shull and M. Van Steenberg, Astrophys. J. Suppl. **48**, 95 (1982).
[24]V. L. Jacobs, J. Davis, P. C. Kepple, and M. Blaha, Astrophys. J. **211**, 605 (1977).
[25]L. J. Roszman, Phys. Rev. A **35**, 2138 (1987).
[26]L. J. Roszman, Phys. Rev. A **35**, 3368 (1987).